Supplementary Material

Relaxed Eddy Accumulation based Flux measurement of Atmospheric Inorganic Acidic Species over Cropland under the Long-Term Exposure to Chemical Industry Emissions in a Chinese Megacity

Jingya Hua, Xinyu Wang, Yulian Wei, Jieya Sun, Zongjun Li, Zhongliang Huang, Qiongqiong Wang, Huan Yu

Department of Atmospheric Science, School of Environmental Studies, China University of Geosciences, Wuhan 430074, China

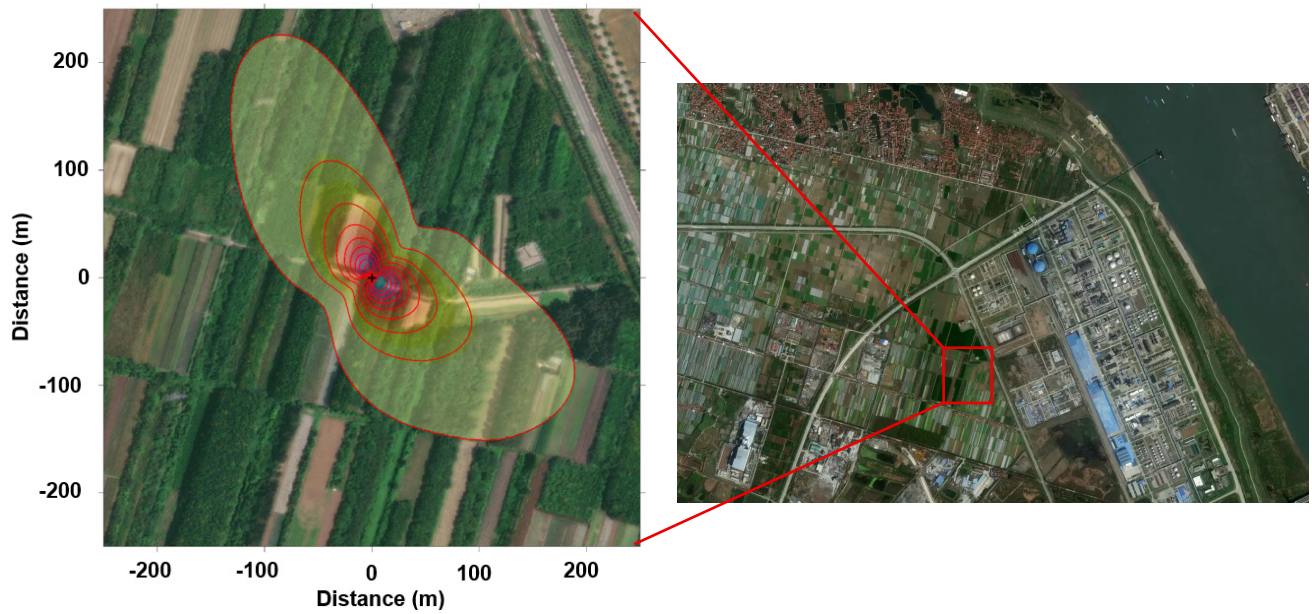

Figure. S1. The cumulative flux footprint during the sampling periods from 29 October to 30 December 2025 at a vegetable cropland adjacent to the Wuhan Chemical Industrial Park. The satellite base map in this figure is sourced from Ovital Map (Omap) and is used for non-commercial academic purpose only.

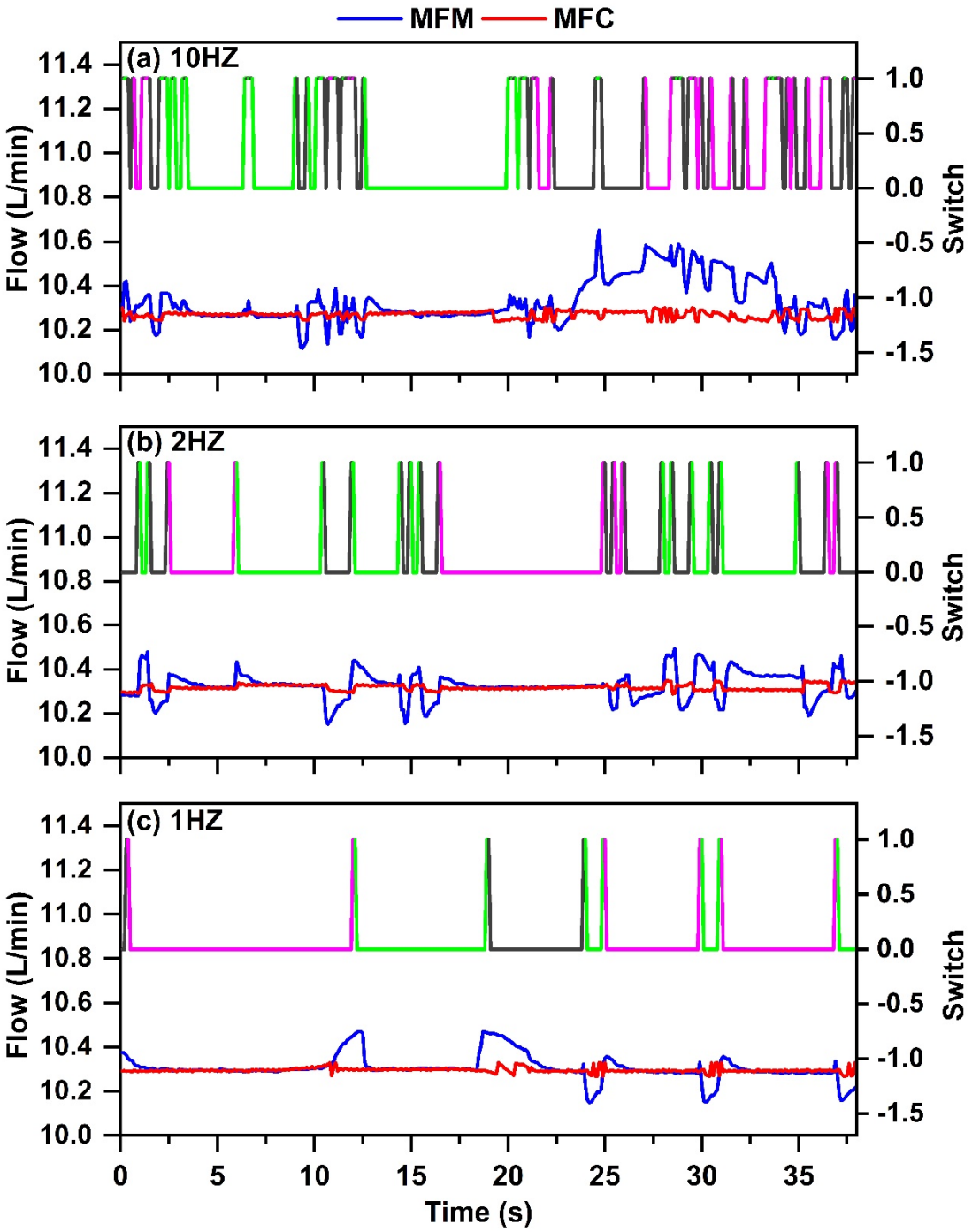

Figure. S2 Flow rate recorded by the on-board mass flow controller (MFC) and the actual flow rate recorded by the calibrated mass flow meter (MFM) mounted temporarily at the sampling inlet, when rapid solenoid valve switched between updraft (green line), downdraft (pink line), and middle (gray line) reservoirs.

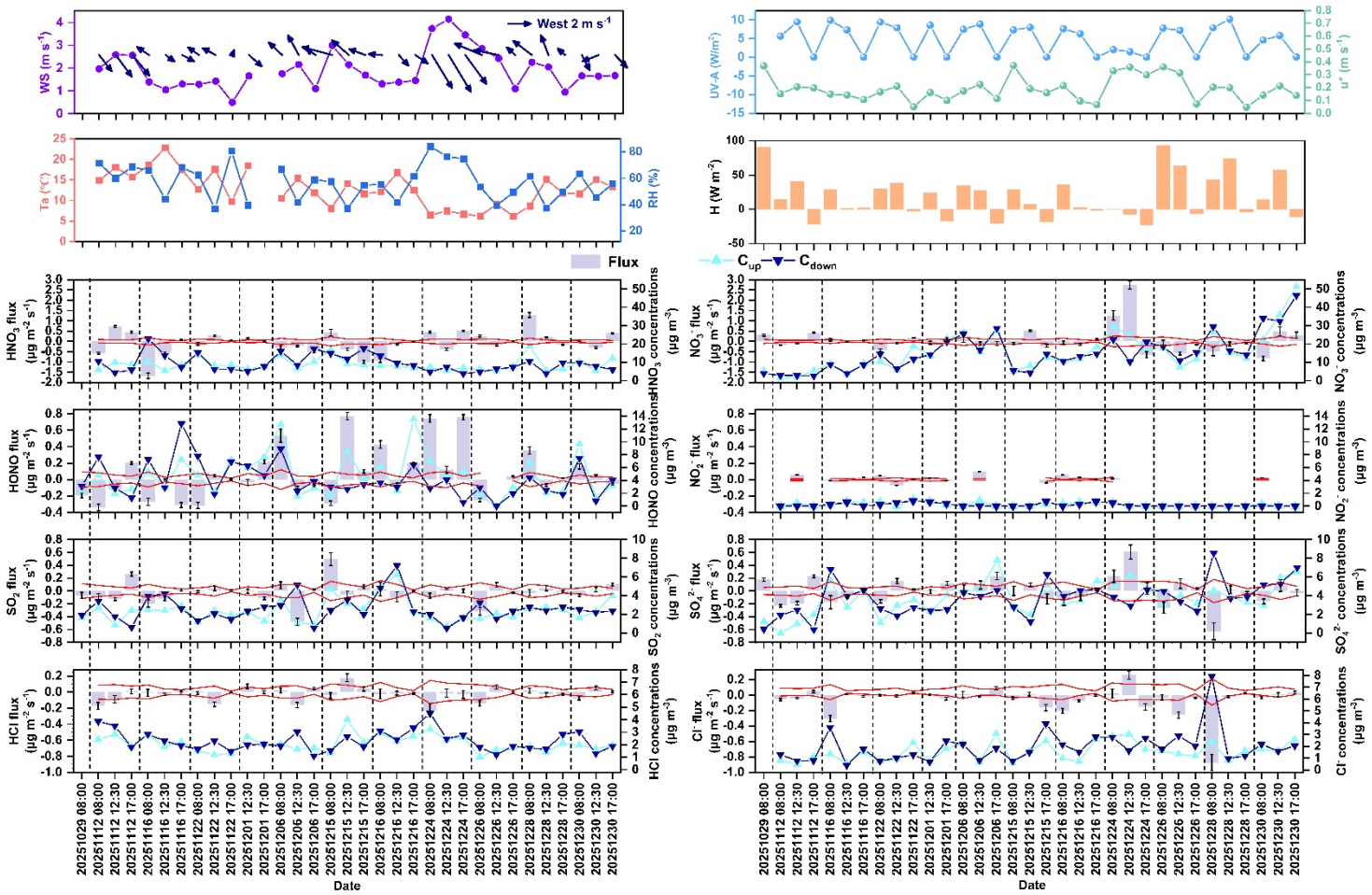

Figure. S3 Time series of wind speed (WS), wind direction (WD), ambient temperature (Ta), relative humidity (RH), ultraviolet-A radiation (UV-A), friction velocity (*u**), sensible heat flux (H), atmospheric inorganic acidic species concentrations in updrafts (C_{up}, light blue lines) and downdrafts (C_{down}, blue lines), and their fluxes (purple columns) during the sampling periods. Error bars indicate the flux precisions, and the red lines are the flux detection limits.

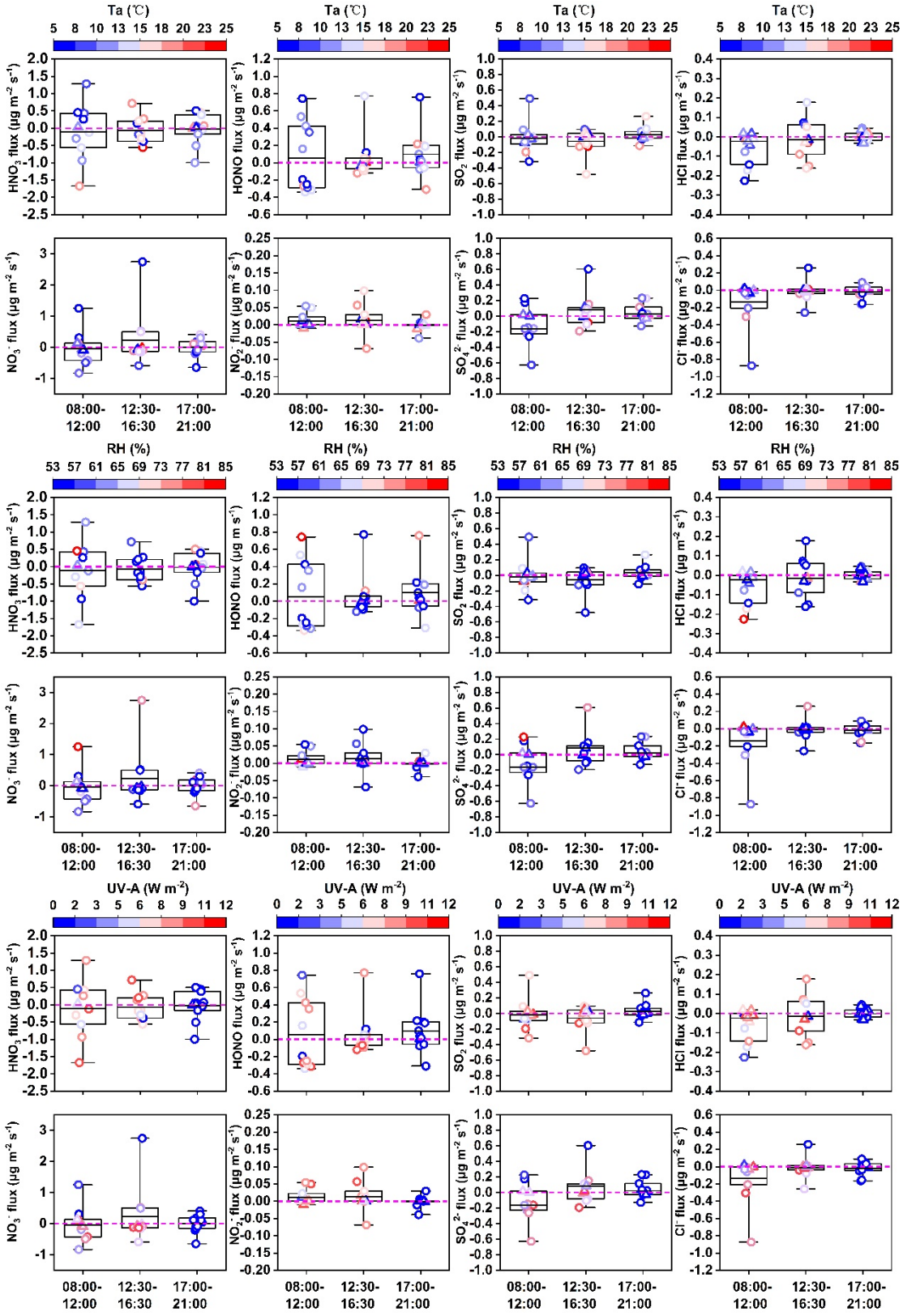

Figure. S4 Box-and-whisker plots overlaid with individual data points showing REA-measured fluxes of eight inorganic species, grouped by diurnal time intervals and coded by Ta, RH, and UV-A from top to bottom. Horizontal lines mark medians, and boxes denote interquartile ranges.

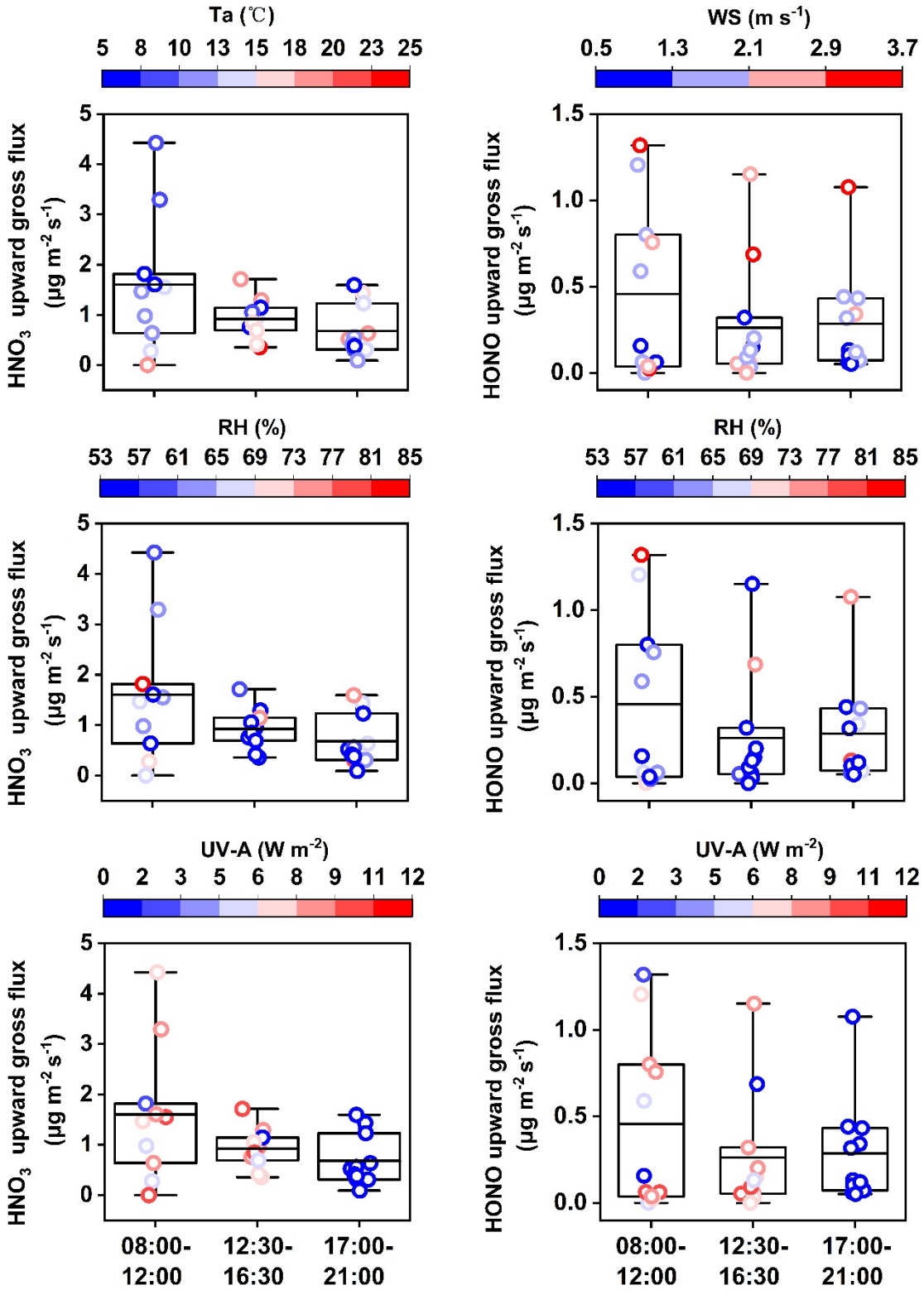

Figure. S5. Box-and-whisker plots overlaid with individual data points showing upward gross fluxes of HNO_3 and HONO, grouped by diurnal time intervals and coded by WS, T_a, RH, and UV-A. Horizontal lines mark medians, and boxes denote interquartile ranges.

Table S1. Simulation results of the relative deviations $\Delta M/M$ of collected HNO_3 mass due to lag time offset Δt = 0.1 s, 0.3 s, and 1.0 s for the 33 runs during the observation campaign.

Relative deviation of M (%.±)	0.1s		0.3s		1s	
	Up	Down	Up	Down	Up	Down
1	5.38	-4.38	17.7	-9.56	5.45	-7.39
2	1.69	-1.68	4.19	-4.26	7.14	-8.22
3	-3.94	3.95	-10.01	10.07	-18.26	19.41
4	-1.64	1.65	-4.20	4.23	-7.55	8.15
5	3.29	-3.28	8.15	-8.32	13.02	-16.04
6	2.82	-2.81	7.01	-7.14	11.48	-13.77
7	-0.75	0.76	-1.95	1.96	-3.47	3.77
8	0.79	-0.78	1.93	-1.96	3.34	-3.78
9	-1.09	1.10	-2.80	2.81	-5.00	5.42
10	-1.09	1.10	-2.80	2.81	-5.00	5.42
11	-0.65	0.66	-1.69	1.70	-3.01	3.27
12	0.07	-0.06	0.12	-0.13	0.20	-0.25
13	0.85	-0.84	2.07	-2.10	3.59	-4.06
14	0.85	-0.84	2.07	-2.10	3.59	-4.06
15	1.59	-1.58	3.95	-4.01	6.75	-7.74
16	-0.76	0.77	-1.98	1.99	-3.52	3.83
17	1.13	-1.12	2.79	-2.83	4.82	-5.47
18	2.44	-2.43	6.07	-6.17	10.10	-11.91
19	2.50	-2.49	6.20	-6.30	10.29	-12.16
20	1.07	-1.06	2.63	-2.67	4.54	-5.15
21	0.52	-0.51	1.26	-1.28	2.19	-2.47
22	-1.61	1.62	-4.10	4.13	-7.37	7.96
23	0.96	-0.95	2.37	-2.41	4.10	-4.65
24	-2.01	2.02	-5.13	5.16	-9.23	9.94
25	-0.73	0.74	-1.90	1.91	-3.38	3.67
26	0.48	-0.47	1.16	-1.18	2.02	-2.28
27	-0.20	0.21	-0.55	0.55	-0.97	1.04
28	-9.80	9.81	-24.88	24.98	-46.30	48.15
29	-0.85	0.86	-2.19	2.20	-3.90	4.24
30	1.27	-1.26	3.14	-3.18	5.39	-6.14
31	-0.01	0.02	-0.09	0.08	-0.17	0.16
32	1.09	-1.08	2.69	-2.73	4.64	-5.27
33	-6.89	6.90	-17.50	17.58	-32.31	33.89